

Electrochemical impedance spectroscopy implementation with L9965x battery management chipset

Introduction

Battery management ICs play an important role in ensuring the safety of users, while making sure they get the most out of their battery-powered devices. Battery management solutions require accurate voltage, current, and temperature measurements to ensure appropriate safety level during battery operations.

ST product portfolio offers a wide set of BMS products targeting different application segments: L9961 (with associated reference boards like STEVAL-L99615C), L9963E and latest L9965x family.

The present document describes an application setup showcasing electrochemical impedance spectroscopy methodology on a 5-cell battery pack using ST L9965x family of highly integrated battery management integrated circuit (BMIC).

Electrochemical impedance spectroscopy methodology is a powerful and widely used non-invasive and non-destructive battery characterization technique based on estimating the impedance of batteries.

It is useful for understanding important information of batteries and their constituent parts.

Figure 1. Example of an EIS setup



Note: For dedicated assistance, submit a request through our online support portal at www.st.com/support.

1 Electrochemical impedance spectroscopy

The electrochemical impedance spectroscopy (EIS) applied to batteries allows the investigation of physical and chemical phenomena using a non-invasive and non-destructive methodology.

This leads to the determination of much important information of batteries like the state of health (SoH), precise estimation of cell internal temperature (increasing safety by preventing thermal runaway) and, in some cases, the state of charge (SoC).

The electrochemical impedance spectroscopy (EIS) is based on the perturbation of an electrochemical system in equilibrium or in steady state, via the application of a signal (AC voltage in potentiostatic mode or AC current in galvanostatic mode) over a wide range of frequencies.

The response (current or voltage, respectively) of the system to the applied perturbation is then measured.

Usually, a small alternating current perturbation signal (or voltage) is superimposed on the direct current bias that mimics the charge or discharge conditions of a cell.

Battery impedance is a frequency-dependent complex number characterized by the ratio of voltage to current and the phase angle shift between them. It is worth noting that, being a complex number, both real and imaginary parts can be used.

$$Z = \frac{V}{I} = Z_0 e^{j\varphi} = Z_0 (\cos\varphi + j\sin\varphi) = Z' + jZ''$$

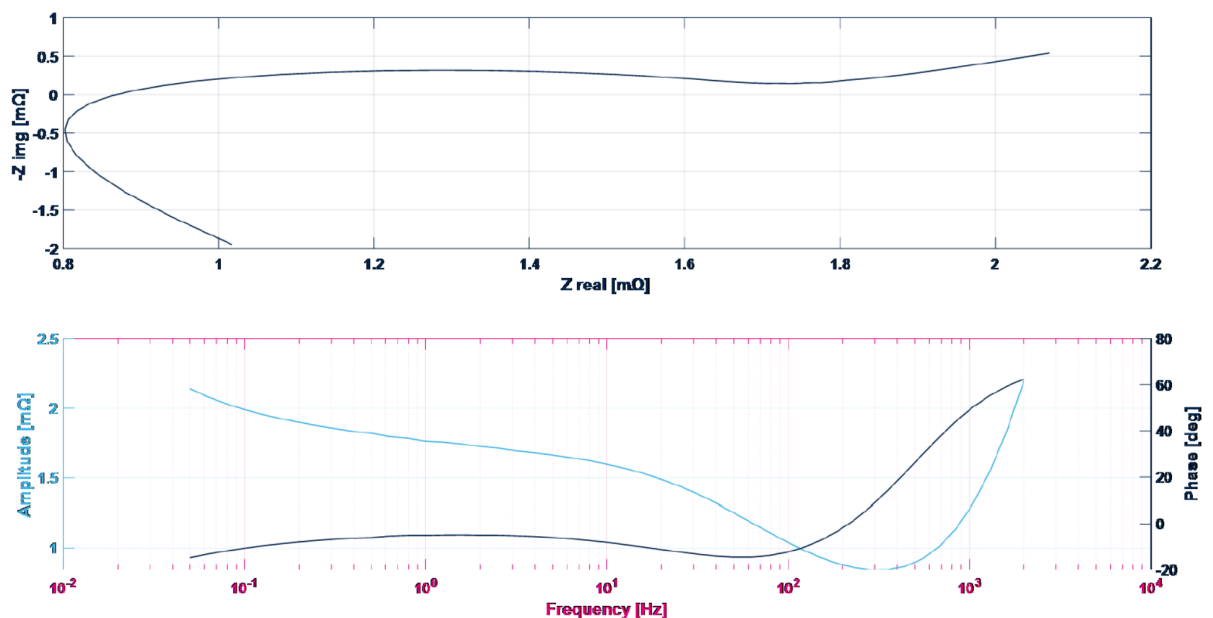
Hence, impedance data can be analyzed by plotting them in different formats. The most widespread are the Nyquist and Bode plots.

In the Nyquist plot, the imaginary part of the impedance is plotted versus the real part of the impedance while in the bode plot two curves provide an easy matching of the excitation frequency with the module of impedance and the phase values.

The Nyquist plot is commonly translated into a Cole-Cole diagram where the imaginary axis is inverted.

By scrolling the plot from left to right, it ranges from high to low frequencies.

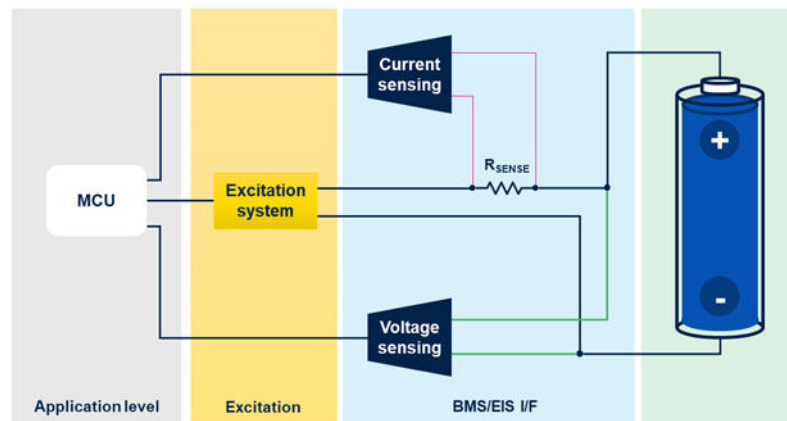
Figure 2. Nyquist and Bode plots



To perform EIS the following building blocks are required:

- Batteries, being the element to be investigated through EIS
- Measurement unit, able to synchronously acquire voltage and current pairs from the perturbed system
- Excitation subsystem, able to provide the right excitation to perturb the batteries at different frequencies
- Postprocessing unit, to put in place algorithm able to evaluate the battery impedance.

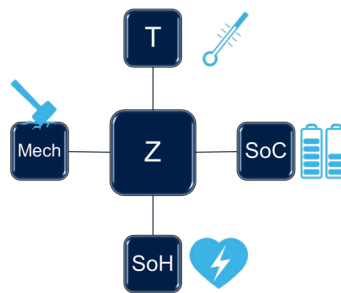
Figure 3. EIS general test setup



1.1 EIS applications

The battery is an electrochemical system, highly influenced by the temperature, the chemical state driven by the state of charge, the usual chemical deterioration often depicted as state of health (SoH) and by external factors such as mechanical stresses.

Figure 4. Impedance correlation

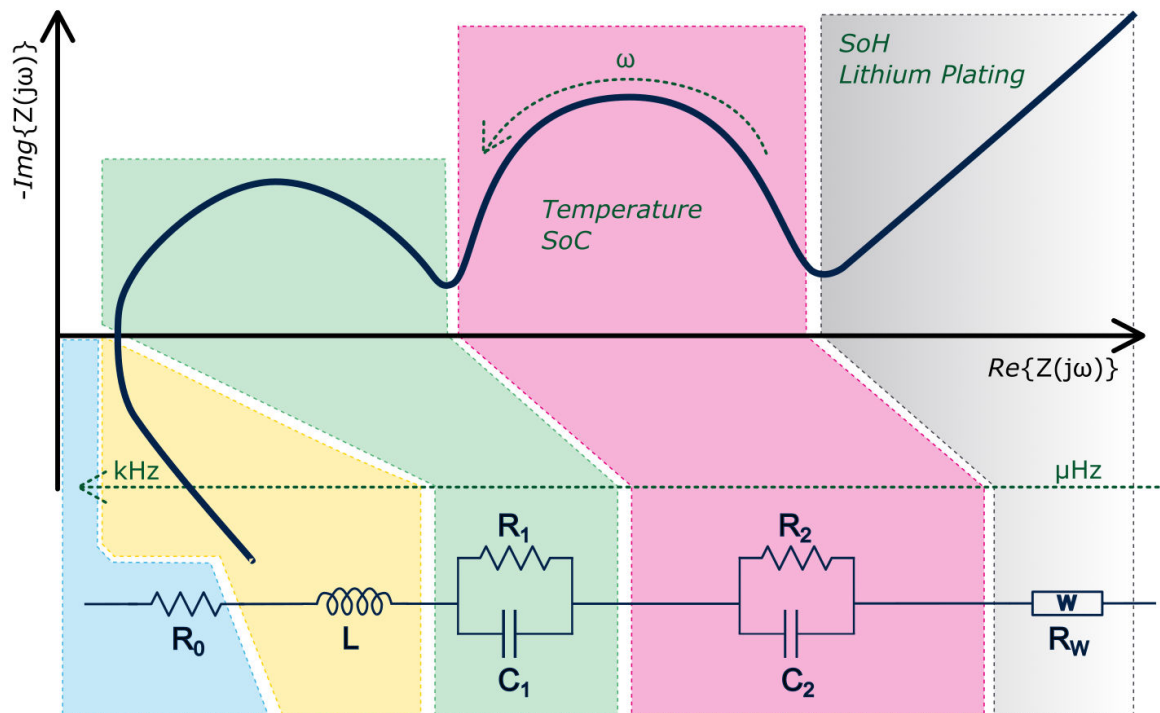


EIS can complement and improve all battery management systems in its common activities like SoC estimation, balancing, charging, temperature monitoring, etc.

It also extends BMS to new functionalities such as SoH and temperature estimation helping in thermal runaway prediction; this increases safety and can potentially reduce costs.

The batteries are nowadays everywhere, so the next innovation step is to provide proper usage of battery impedance measurements.

Figure 5. Nyquist diagram with associated ECM (below) and electro-chemical information (green)



The Figure 5 shows a theoretical Nyquist diagram, with each section corresponding to an electrical component of the battery's equivalent circuit model (ECM). The ECM translates key electrochemical phenomena (green text) into circuit elements, enabling quantitative analysis of the battery's internal processes

Low-frequency impedance is correlated with the SoH of the battery and, particularly, with the degradation phenomena of lithium plating.

Lithium plating occurs when metallic lithium deposits on the anode surface during charging, which can reduce battery capacity and increase safety risks such as short circuits.

The two semicircles, usually merged into one, correspond to charge transfer and double-layer capacitance processes at the electrode-electrolyte interfaces.

These processes govern the kinetics of energy storage and release in the battery. Consequently, the diameter and shape of these semicircles are influenced by the battery's temperature and SoC, as both parameters affect reaction rates and ion diffusion within the cell.

Another critical feature in the nyquist plot is the point where the impedance curve crosses the real axis, where the imaginary part changes from negative to positive. This intercept is correlated with the battery's internal temperature because temperature variations affect the electrolyte conductivity and charge transfer resistance.

Monitoring this crossing point allows for non-invasive estimation of the cell's thermal state, which is crucial for battery management systems aiming to optimize performance and ensure safety.

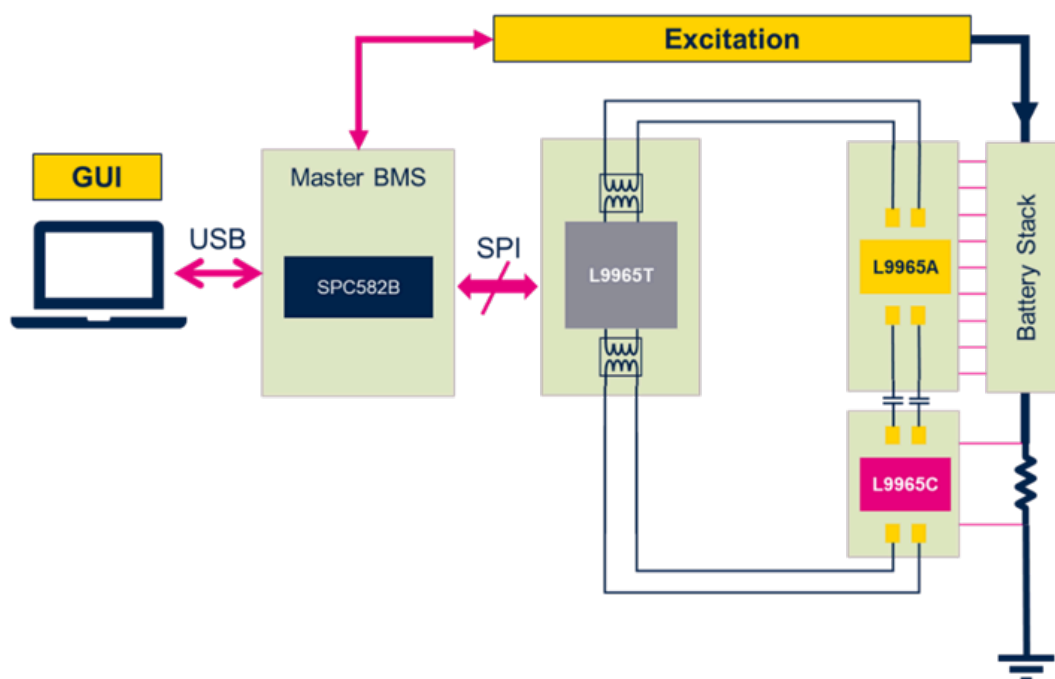
The frequency range for performing EIS is related to the batteries used. Looking at the Nyquist diagram, the measurement loses importance for values of imaginary impedance below zero as well as above the so-called Warburg impedance.

In general, the higher the capacity, the lower the crossing frequency at the point where the imaginary impedance is zero.

2 System overview

The proposed setup is entirely based on ST products, both hardware and software. This system has been built to show EIS performance of ST products, especially of the L9965x family. This setup is performing EIS on five series-connected cells.

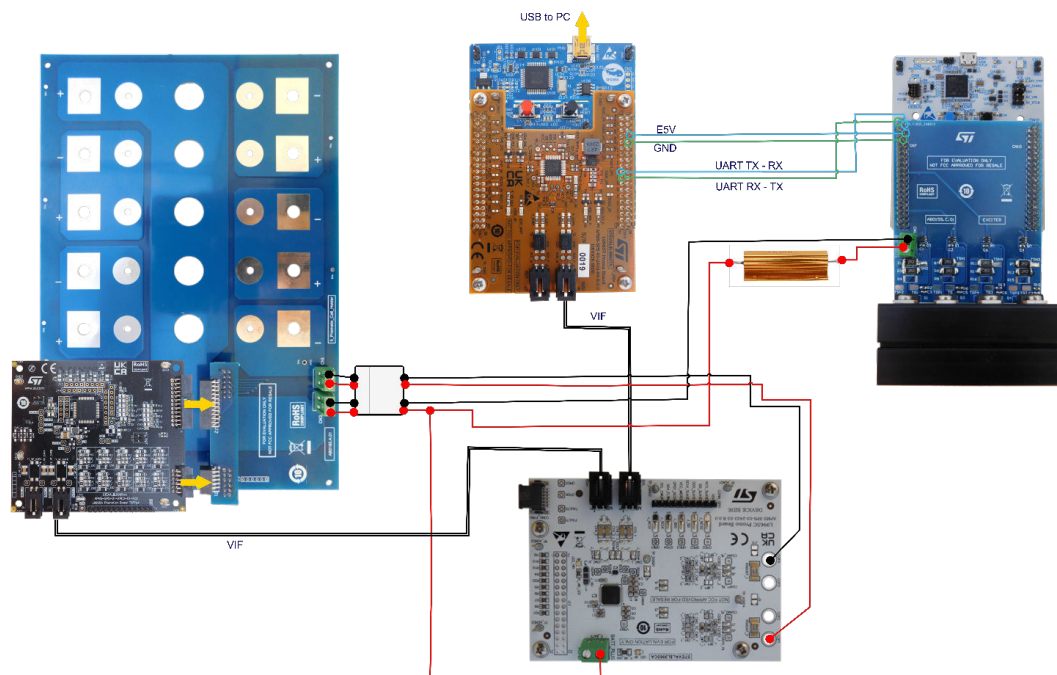
Figure 6. System block diagram



In the block diagram of the overall system (Figure 6), the battery stack, the excitation section and the master BMS are clearly arranged, highlighting their interaction with each other as well as with the three main integrated circuits (ICs) forming the acquisition section: L9965T, L9965A, L9965C.

A MATLAB graphical user interface (GUI) has been used for application configuration by sending the appropriate commands, as well as for visualization of the Nyquist curves thus obtained.

An excitation system performing galvanostatic excitation has been built using STM32G474x Nucleo board.

Figure 7. EIS implemented architecture


2.1 Battery holder

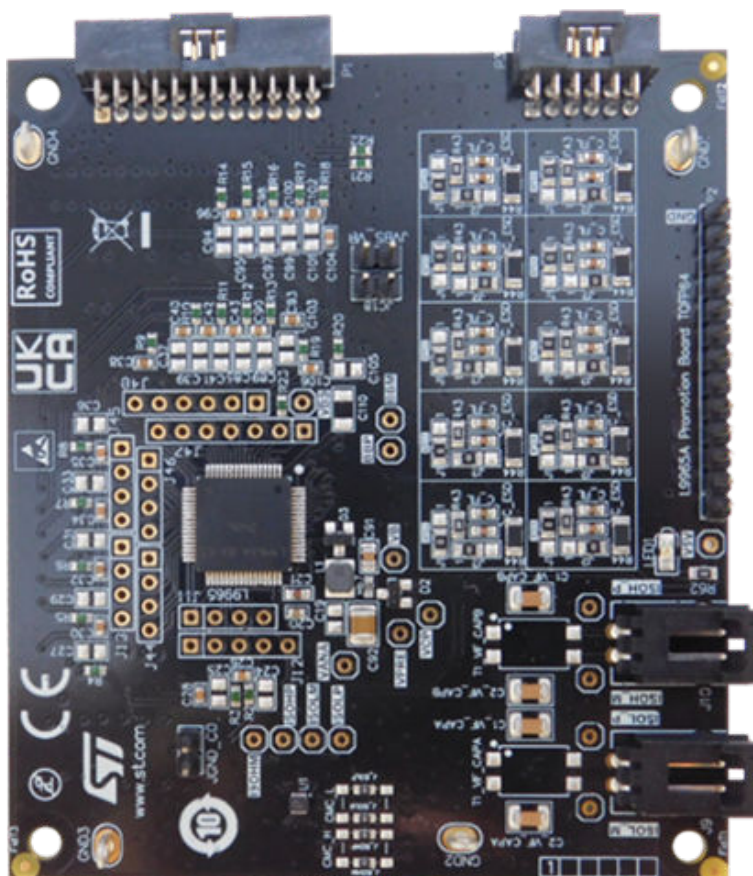
A dedicated battery holder has been designed to properly connect different battery types to the setup. This is a key element of any battery pack and is more often referred as cell contact system (CCS), battery connection unit (BCU) or many other equivalent names.

2.2 Measurement interface

The interface to the batteries is made by **L9965A** and **L9965C** boards handling synchronous voltage and current acquisition.

The **Figure 8** shows a HW tool for the evaluation of the **L9965A** chip. This IC enables ASIL-D on cell voltage measurement, temperature measurement and communication in both normal and low power states, featuring a comprehensive set of cell/pack monitoring, balancing, and protection functions.

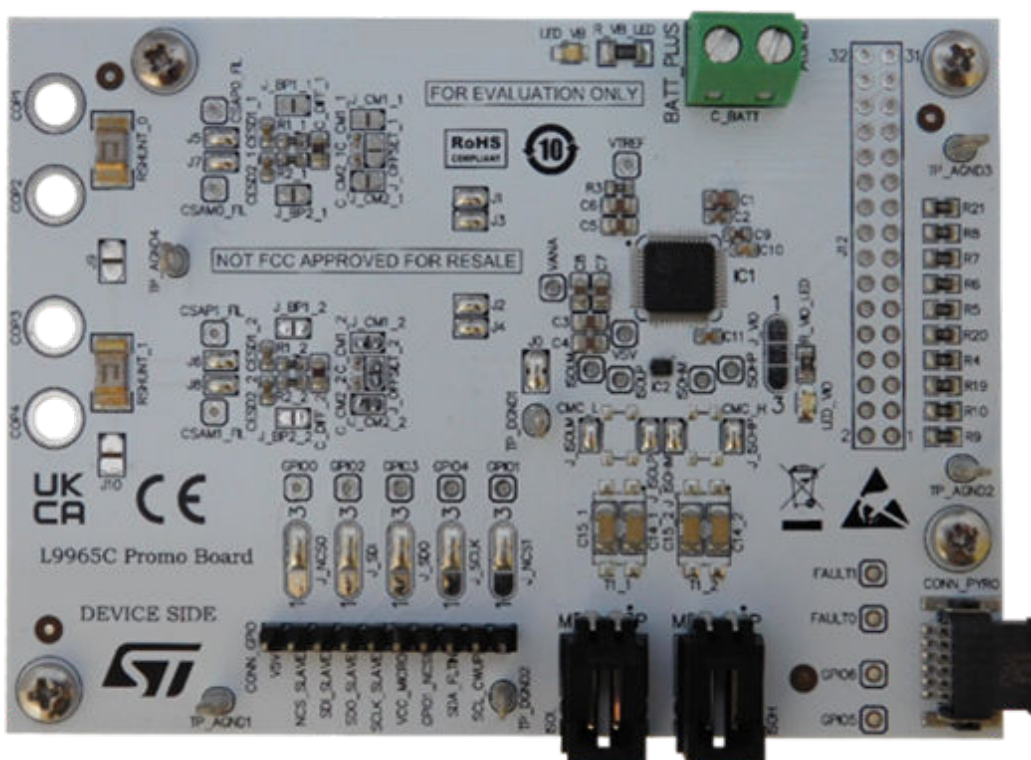
Figure 8. L9965A application board example



The **L9965A** synchronously acquires cell, busbar, and pack voltage in configuration of up to 18 cells, **L9965A** also monitors cells and battery pack voltage with independent ADCs: one ADC per cell, one dedicated to the busbar and one for battery stack voltage through an appropriate measurement pin.

The **Figure 9** shows a HW tool for the evaluation of the **L9965C** chip. This device implements ASIL-D current sensing with short-circuit/overcurrent protection alongside voltage, charge and isolation monitoring pre-charge control algorithm for HV battery packs.

Figure 9. L9965C application board example



The **L9965C** monitors instantaneous pack current by means of an external shunt resistor, providing current measurements synchronized with battery cell voltages as well as instantaneous power information and detecting overcurrent and short-circuit events. Current is also integrated over time to accumulate pack charge information according to the well-known coulomb counting algorithm.

There are two pairs of current sense amplifiers (CSA) pins, implementing a fully differential and redundant sensing architecture.

The first one is used for sensing the instantaneous pack current while the second one is used for performing coulomb counting.

2.3 Excitation

An excitation circuit, like the one in [Figure 10](#) , provides an excitation AC current of up to 10 A across a wide frequency range.

In the proposed setup the excitation is carried out locally at module level with a passive excitation based on four identical parallel channels based on an operational amplifier.

This setup ensures proper current flowing from the battery pack through MOSFETs by means of a DAC input signal provided by STM32G474x Nucleo board.

Figure 10. Exciter



2.4 Processing

The SPC582B MCU is working as a BMS master. It performs all BMS functionalities and offers a virtual COM port channel to communicate with MATLAB GUI allowing user interaction.

The SPC582B-DIS discovery board is an evaluation tool supporting STMicroelectronics SPC582B60E1 chorus 1M, a high performance e200z2 single core 32-bit power architecture technology CPU 80 MHz, 1088 KB (1024 KB code flash + 64 KB data flash), 96 KB SRAM in an eTQFP64 package. It supports ASIL-B requirements.

An ST patented algorithm is used to measure the battery impedance.

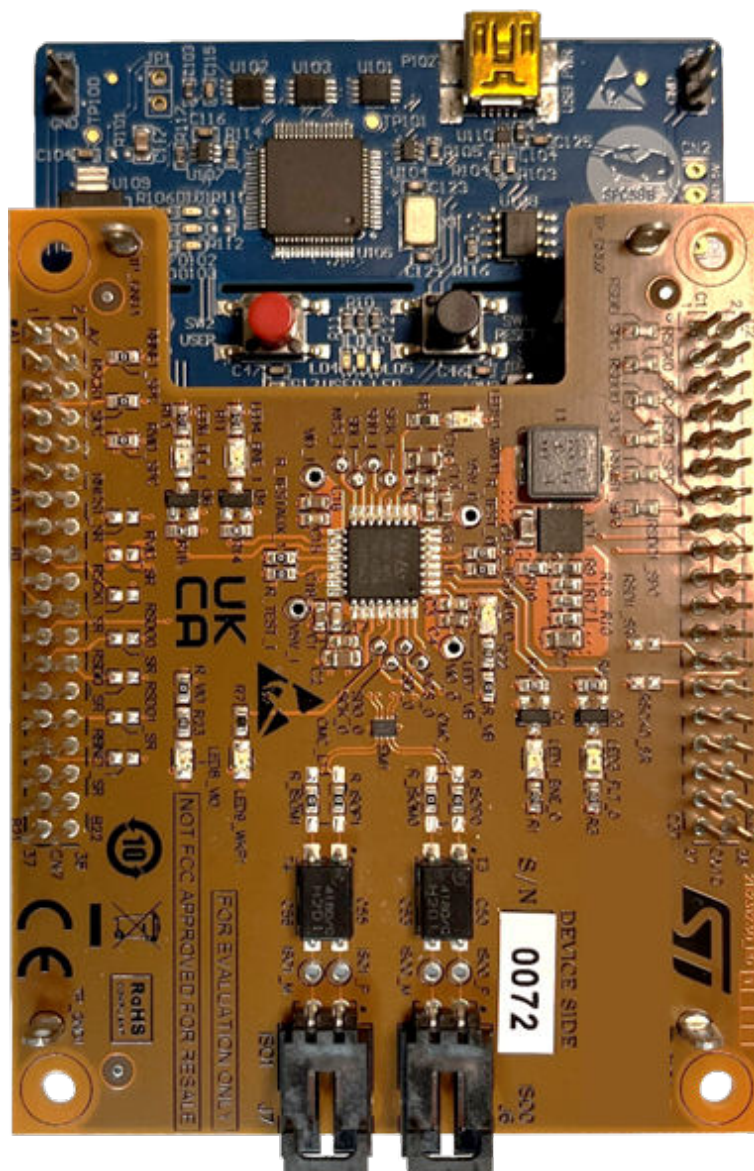
Hardware for L9965T is plugged into SPC582B-DIS ,[Figure 11](#) , offers an SPI to isolated SPI transceiver to enable a communication bridge between devices located into different voltage domains.

L9965T transceiver converts data incoming from a classical 4-wire based SPI interface to a 2-wire isolated interface known as vertical interface (VIF), and vice versa.

Through the VIF, the BMS master can access all the daisy-chained L9965x devices in different voltage domains. Broadcast write commands allow simultaneous writing on all devices or a subset of them. At the same time, a flexible burst read mode (standard or compressed) is implemented on the VIF to enable quick data retrieval from the chained devices.

In the proposed setup, ST's "4-points" algorithm is used to evaluate impedance. This algorithm based on sinusoidal battery excitation is able to run online with both a negligible memory footprint (i.e. compared to fft) and a reduced computational effort.

Figure 11. SPC582B-DIS and L9965T example board

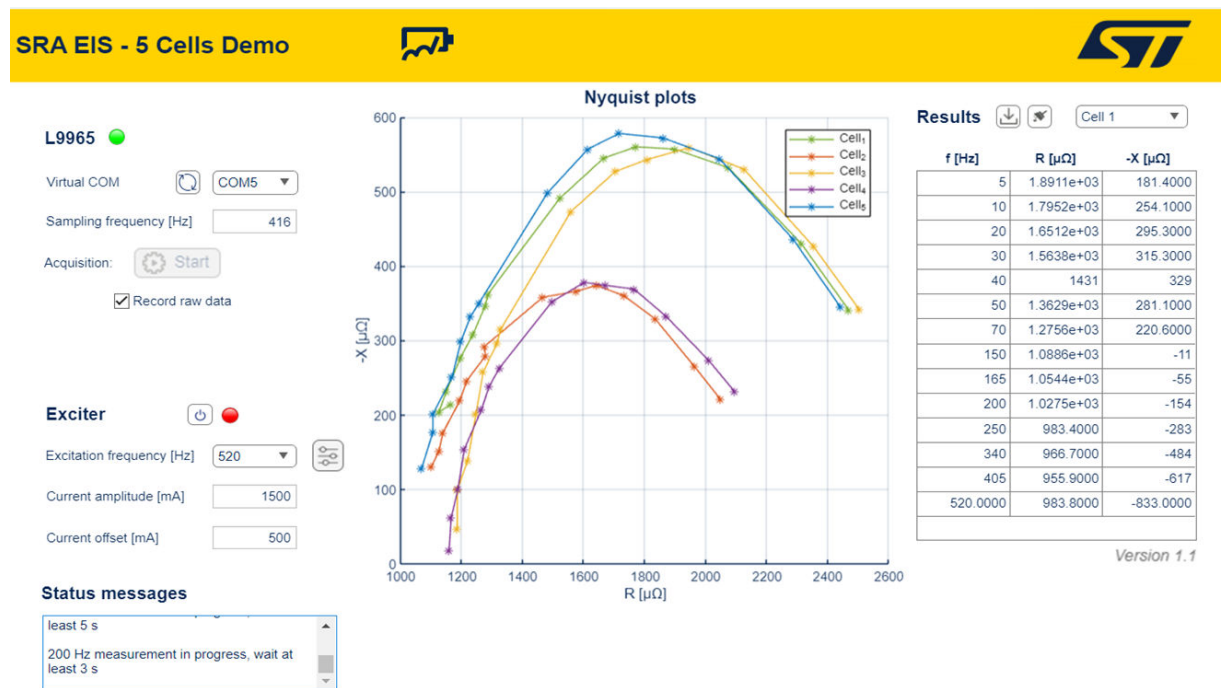


3 Test performed

Test performed for this application uses five batteries with an excitation range from 5 Hz to 520 Hz with three A_{pp} on 32 Ah li-ion prismatic cell batteries.

The GUI, shown in Figure 12, has been developed to interact with the BMS master in the proposed setup taking care of performing proper actions.

Figure 12. MATLAB GUI



Once that excitation parameters are selected, a start function drives interaction with the BMS master to execute impedance measurement and, after data collections, to produce a Nyquist diagram of the five battery impedances.

4 Results

In Figure 13, Figure 14 and Figure 15, results obtained from a 32 Ah li-ion prismatic cell (single cell analysis within the battery pack of five cells) are presented. The figure includes a Bode plot highlighting amplitude with respect to frequency, a bode plot highlighting phase, and a Nyquist plot.

Figure 13. Bode amplitude

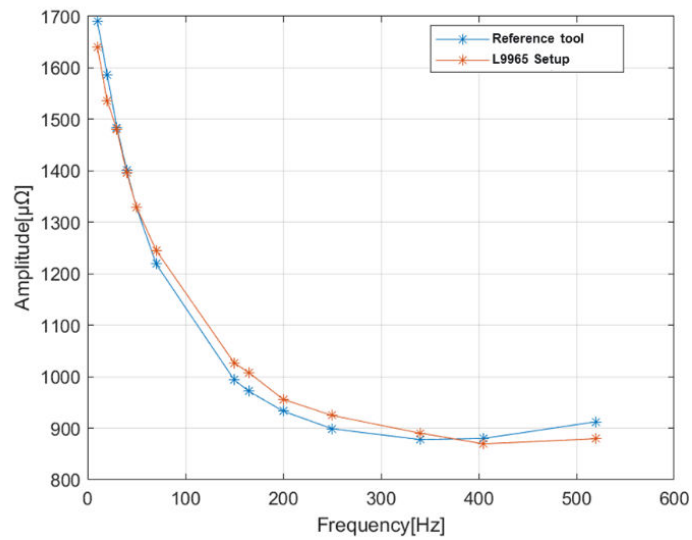


Figure 14. Bode phase

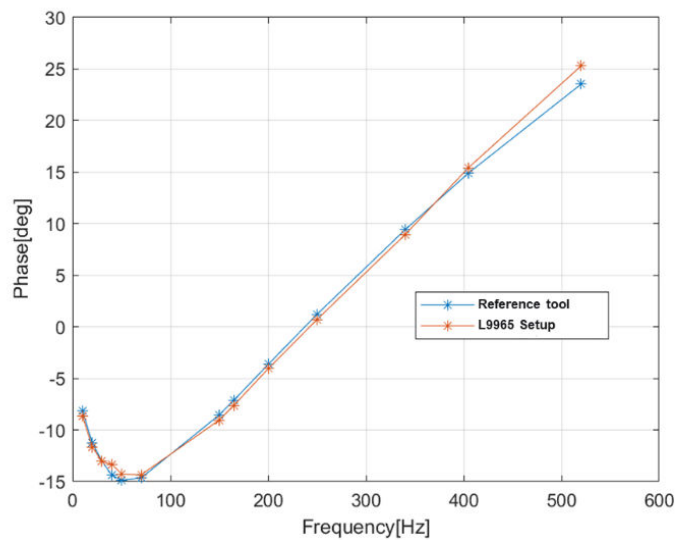
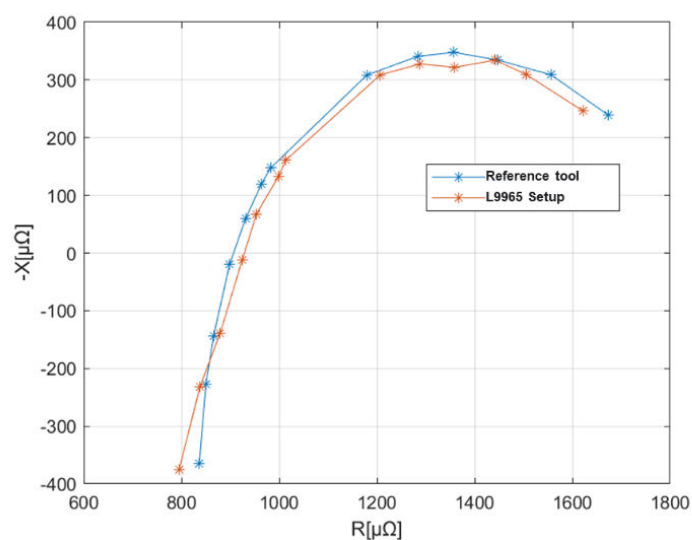


Figure 15. Nyquist plot



Curves obtained with this EIS demonstrator setup are compared to those obtained using a galvanostat measuring instrument, confirming a minimal error of about $24 \mu\Omega$ for Bode amplitude, 0.6° for Bode phase and $29 \mu\Omega$ for Nyquist (values for the single cell shown in Figure 13, Figure 14 and Figure 15).

Revision history

Table 1. Document revision history

Date	Revision	Changes
16-Sep-2025	1	Initial release.

Contents

1	Electrochemical impedance spectroscopy	2
1.1	EIS applications	3
2	System overview	5
2.1	Battery holder	6
2.2	Measurement interface	7
2.3	Excitation	9
2.4	Processing	9
3	Test performed	11
4	Results	12
	Revision history	14
	List of figures	16

List of figures

Figure 1.	Example of an EIS setup	1
Figure 2.	Nyquist and Bode plots	2
Figure 3.	EIS general test setup	3
Figure 4.	Impedance correlation	3
Figure 5.	Nyquist diagram with associated ECM (below) and electro-chemical information (green)	4
Figure 6.	System block diagram	5
Figure 7.	EIS implemented architecture	6
Figure 8.	L9965A application board example	7
Figure 9.	L9965C application board example	8
Figure 10.	Exciter.	9
Figure 11.	SPC582B-DIS and L9965T example board	10
Figure 12.	MATLAB GUI	11
Figure 13.	Bode amplitude	12
Figure 14.	Bode phase	12
Figure 15.	Nyquist plot	13

IMPORTANT NOTICE – READ CAREFULLY

STMicroelectronics NV and its subsidiaries ("ST") reserve the right to make changes, corrections, enhancements, modifications, and improvements to ST products and/or to this document at any time without notice.

In the event of any conflict between the provisions of this document and the provisions of any contractual arrangement in force between the purchasers and ST, the provisions of such contractual arrangement shall prevail.

The purchasers should obtain the latest relevant information on ST products before placing orders. ST products are sold pursuant to ST's terms and conditions of sale in place at the time of order acknowledgment.

The purchasers are solely responsible for the choice, selection, and use of ST products and ST assumes no liability for application assistance or the design of the purchasers' products.

No license, express or implied, to any intellectual property right is granted by ST herein.

Resale of ST products with provisions different from the information set forth herein shall void any warranty granted by ST for such product.

If the purchasers identify an ST product that meets their functional and performance requirements but that is not designated for the purchasers' market segment, the purchasers shall contact ST for more information.

ST and the ST logo are trademarks of ST. For additional information about ST trademarks, refer to www.st.com/trademarks. All other product or service names are the property of their respective owners.

Information in this document supersedes and replaces information previously supplied in any prior versions of this document.

© 2025 STMicroelectronics – All rights reserved